Author Manuscript

Published in final edited form as:

Clin Biomech (Bristol, Avon). 2018 Feb;52:72-78.

Doi: 10.1016/j.clinbiomech.2018.01.005.

Title:

BIOMECHANICAL EVALUATION OF PYROCARBON PROXIMAL INTERPHALANGEAL JOINT ARTHROPLASTY: AN IN-VITRO ANALYSIS

Completo A[1], Nascimento A[2], Girão A. F.[1], Fonseca F[2]

[1] Mechanical Engineering Department, University of Aveiro, Portugal

[2] Orthopaedics Department, Coimbra University Hospital, Portugal

Abstract

Background

Pyrocarbon proximal interphalangeal (PIP) joint arthroplasty provided patients with excellent pain relief and joint motion, however, overall implant complications have been very variable, with some good outcomes at short-medium-term follow-up and some bad outcomes at longer-term follow-up. Implant loosening with migration, dislocation and implant fracture were the main reported clinical complications. The aim of the present work was to test the hypothesis that the magnitude PIP joint cyclic loads in daily hand functions generates stress-strain behaviour which may be associated with a risk of pyrocarbon component loosening in the long-term.

Methods

This study was performed using synthetic proximal and middle phalanges to experimentally predict the cortex strain behaviour and implant stability considering different load conditions for both intact and implanted states. Finite element models were developed to assess the structural behaviour of cancellous-bone and pyrocarbon components, these models were validated against experimentally measured cortex strains.

Findings

*C*ortex strains showed a significant increase at dorsal side and reduction at palmar side between intact and implanted states. Cancellous-bone adjacent to the condylar implant base components suffers a two to threefold strain increase, comparing with the intact condition.

Interpretation

The use of pyrocarbon implant changes the biomechanical behaviour of the joint phalanges and is associated with a potential risk of support cancellous-bone suffer fatigue failure in mid to long term due to the strain increase for cyclic loads in the range of daily hand activities, this risk is more prominent than the risk of bone resorption due to strain-shielding effect.

Keywords: experimental strains; finite element model; PIP joint; stress-shielding

Introduction

The proximal interphalangeal (PIP) joint is the third most common site of osteoarthritis in the hand (Drake and Segalman, 2010; Haugen et al., 2011). Pinch and grip strength may be substantially reduced as a consequence of pain or limited mobility in this joint. Three surgical procedures are currently used to treat osteoarthritis of the PIP joint: arthrodesis, silicone arthroplasty, and resurfacing arthroplasty with metal-plastic and pyrolytic carbon (pyrocarbon) implants (Adkinson et al, 2014; Ceruso et al., 2017). Pyrolytic carbon implants consist of a graphite core coated with pure carbon with an elastic modulus similar to cortical bone, which has been shown to be biocompatible and to have excellent wear characteristics (Cook et al., 1998; Leuer et al., 1996). The semiconstrained pyrolytic carbon implant for the PIP joint was approved in 2000 for use in Europe and in 2002 in the United States. Most of retrospective clinical studies found that pyrocarbon PIP joint arthroplasty provided patients with excellent pain relief overall and maintained their preoperative PIP joint motion; however, overall implant complications has been very variable, with some good outcomes at short-medium-term follow-up (Branam et al, 2007; Bravo et al, 2007; Chung et al, 2009; Desai et al., 2014; Mashhadi et al, 2012; McGuire et al, 2012; Watts et al., 2012) and some bad outcomes at medium-longer-term follow-up (Chan et al., 2013; Daecke et al., 2012; Dickson et al., 2015; Hutt et al., 2012; Ono et al., 2012; Reissner et al., 2014; Squitieri and Chung, 2008; Sweets and Stern, 2011). Implant loosening with migration, dislocation and implant fracture were the main reported clinical complications (Chan et al., 2013; Ceruso et al., 2017; Dickson et al., 2015; Sweets and Stern, 2011; Reissner et al., 2014). Studies on the structural biomechanics of PIP pyrolytic carbon arthroplasty are very limited. The hypothesis considered in this study is that the magnitude PIP joint cyclic loads in daily hand functions generates stress-strain behaviour which may be associated with a risk of pyrocarbon component loosening in the long-term. Ideally, bone strain values should be low enough to avoid exceeding

fatigue levels of materials, but also, must not be below strain-shielding inductive levels, which lead to significant bone atrophy, ultimately resulting in implant loosening. This study uses synthetic phalanges to experimentally predict cortex strain behaviour and implant stability for different load conditions. In addition, finite element (FE) models were developed to assess the structural behaviour of cancellous-bone around the implant, these models were validated against experimentally measured cortex strains.

Methods

Five synthetic proximal and middle index phalanges bones were manufactured since they were not commercially available (Figure 1). The proximal and middle index phalanges structures were identical, with a foam core to mimic cancellous-bone and a shell of glass fibre and epoxy resin to mimic cortical-bone (Figure 1). The bone cortical geometry was obtained from CT scans of the left hand of a 52 year old man, that were converted to 3D models with an image processing software (ScanIP, Simpleware Ltd. Exeter, UK). The foam core was obtained by CNC machining of blocks of solid rigid polyurethane foam (mod. 1522-03, Pacific-Research-Labs, WA, USA), which provides a consistent and uniform material with properties in the range of human cancellous-bone (ASTM F-1839-08 (2012)). Then, the foam core was layered with short-glass-fiber-reinforced epoxy resin until a mean thickness of 1.1 mm was achieved, in agreement with the mean cortical thickness observed in the CT scans. Four triaxial strain gauges (KFG-3-120-D17-11L3M2S, Kyowa, Japan) were glued on the proximal (Pr) and middle (Mi) index phalanges cortex at the dorsal (Pr_D, Mi_D) and palmar (Pr_P, Mi_P) sides, before prosthesis insertion (Figure 1). The positions of the strain gauges were measured using a 3D coordinate measuring machine. The proximal (30P) and middle (30D) phalanx base components of the PyroCarbon PIP joint prosthesis (Ascension Orthopaedics, Austin, Texas) were implanted by an experienced

surgeon (Figure 1), according to the protocol described for this prosthesis (Surgical technique Ascension PIP Total Joint Replacement, 2016). Applied loads were obtained from the bibliography, as reasonable estimates of PIP joint loads from index finger for three isometric hand functions: Tip Pinch, Key Pinch and Pulp Pinch (Table 1) (An et al. 1985; Fok and Chou, 2010; Fowler and Nicol, 2000). Six experimental load-cases were applied, result from three PIP joint flexion angles (15º, 35º and 50º) with two joint constraint forces (Table 1). The distal middle phalanx region was rigidly fixed (Figure 1). In order to establish correlations with FE models and evaluate the risk of failure of the supporting cortex, the maximum-ε1 and minimum-ε2 principal strains within the plane of the gauge were calculated and averaged, and the standard deviations determined. Normal distribution of all data was evaluated through an exploratory data analysis. Paired t-tests were performed to assess the statistical significant difference of the mean principal strains. The initial proximal and middle implant components stability was evaluated after 25,000 load cycles at a frequency of 1Hz through a pull-out movement.

Finite element analysis

Finite element (FE) models of intact and implanted PIP joint were made from CT-scans of the experimental models, which were then converted to 3D models with an image processing software (ScanIP, Simpleware Ltd. Exeter, UK). The implant models were created with a CAD modelling package (Catia, Dassault-Systèms, France). The FE meshes were built from 10-node second-order tetrahedral elements (C3D10). The number of elements were chosen based on convergence tests of the maximal displacement and the minimal principal strains at 2 locations (dorsal and palmar sides). The convergence rate of the displacements was less than 0.7% and less than 3% for the minimal principal strains when nearly 46000 elements were used. Non-linear contact formulation analysis was performed with ABAQUS (6.12-1) (Providence, USA). The bone-pyrocarbon interface was modelled with a finite sliding surface-to-surface contact algorithm with a coefficient

of friction of 0.15 (Grant et al., 2007; Stanley et al., 2008). The material properties used were those described by the manufacturer (Table 2) and were assumed to be homogeneous, isotropic and linear elastic. Regression analyses between the principal strains predicted by the FE models and experimentally measured strains were performed. The overall absolute difference between numerical and experimental cortex strains, the root-mean-square-error was calculated and expressed as a percentage of the peak values of the measured principal strains (RMSE %). The same load-cases were used to analyse principal cancellous-bone strains before and after implantation, as well as von Mises stresses in the pyrocarbon prosthesis components.

Results

The means and standard deviations of the cortex principal strains for each strain gauge are depicted in Figure_2 for the six load cases, where it is possible to see that the average standard deviation of the principal strain was less than 11%. The six load cases analysed presented similar cortex strain behaviour between intact and implanted states, with an strain increase at the dorsal strain gauges (Pr_D, Mi_D) and reduction at the palmar strain gauges (Pr_P, Mi_P). The Key Pinch (load case 2 and 4) presented the highest principal strains of all load cases analysed. The magnitude of minimal principal strains was greater than maximal principal strains, with the highest values measured on the Proximal Palmar (Pr_P) and Middle Dorsal (Mi_D) strain gauges. Significant ($p<0.05$) minimum principal cortex strain reduction at the palmar and increase at the dorsal strain gauges between intact and implanted states were observed for all load cases (Table 3). After 25,000 load cycles (1Hz) both pyrocarbon components presented good stability without any sign of slippage/release during the pull-out movement. The linear regression correlation value (R^2) was 0.96 and the slope was 1.03 (Figure_3). The overall absolute difference between numerical and experimental cortex strains (RMSE %) was 15%. Figure_4 shows the patterns of the minimum

principal strains in cancellous bone obtained in the FE analysis. For all load cases the implanted state increased two to threefold cancellous-bone strains near to the condylar surfaces region, while at the palmar side cancellous-bone strain dropped on average to half relatively the intact case. The highest pyrocarbon implant stress was reached in the Key Pinch (load case 5) with 66.8 MPa (Table 4).

Discussion

The aim of the present work was to investigate in-vitro implant–bone load transfer mechanisms with the Ascension PIP Pyrocarbon prosthesis. To the authors' knowledge there are no other studies comparing stress-strain levels in intact and implanted PIP joint with a pyrocarbon implant, neither in-vitro nor using the FE method. The standard deviations of the measured cortex strains were within the range of those found in the literature which used other synthetic bones (Completo et al., 2010; Completo et al., 2011, Meireles et al., 2010). The average of the cortex principal strains in the implanted PIP joint presented a significant reduction ($p<0.05$) relatively to the intact joint at the palmar side, while at the dorsal side a significant cortex strain increase ($p<0.05$) was observed. These experimental results shows that the PIP joint is not immune to using a pyrocarbon prosthesis. The FE models developed to analyse cancellous-bone, major support structure for the implant, presented correlation, slope, intercept values of the linear regressions and RMSE values in the range of other previous experimental-numerical studies performed with synthetic bones (Completo et al., 2013; Completo et al., 2008; Heiner, 2008), which reveals a good agreement between FE and measured strains. As observed experimentally at the cortex, cancellous bone strain behaviour in the implanted PIP joint was very different of intact state for all load-cases analysed. In the implanted case the condylar region, of both phalanges, suffers a pronounced strain increase (two to threefold) comparing with the intact condition. Therefore, the strain increase indicates a

potential risk of cancellous-bone fatigue failure for both phalanges due to cyclic loads; bone can suffer fatigue failure if the induced strain approaches 60 to 80% of the yield strain (Choi and Goldstein, 1992). These strain levels may occur if the normal maximum compressive strains in the cancellous bone of the intact joints are increased by 50 to 100% due to implantation (Burstein and Wright, 1994), which is the present case. The cancelous-bone strain reduction, about 50%, at the palmar side for both phalanges point to a limited risk of bone resorption due to strain-shielding effect (Gross and Rubin 1995; Frost, 2003). The maximum von Mises stress values reached at the pyrocarbon prosthesis are below the fatigue limit (Ma and Sines, 2000), which represents a reduced risk of implant fracture. All these stress-strain results reveal mainly a potential risk of fatigue failure of support cancellous-bone due to cyclic loads, which is enhanced by the magnitude of joint loads as well as by the number of load cycles. This potential risk may be related with several clinical mid-long term outcomes that evidence the ongoing migration, dislocation, tilt and potential failure Ascension PyroCarbon prosthesis (Chan et al., 2013; Ceruso et al., 2017; Dickson et al., 2015; Reissner et al., 2014; Sweets and Stern, 2011). Limiting the magnitude of index finger forces after arthroplasty can contribute positively to reduce the overload effect in the cancellous-bone adjacent to the pyrocarbon implant reducing the risk of fatigue failure of the support bone.

As in all experimental-numerical studies, the present study had some shortcomings, one such limitation is concerned with the use of synthetic bones and experimental simplifications required to represent the functioning pyrocarbon PIP implant. The advantage of using artificial bones is that specimen geometry is constant, which optimizes the reproducibility of results obtained in tests.

Experimental load-cases were simplified in terms of applied loads and structural links (ligaments, muscles, etc.), however, applied load-cases are representative of major loads acting upon the implant and bone structure, furthermore, due to the comparative nature of the study, it is concluded

that the observed strain results are representative of major differences between intact and implanted states.

Conclusions

The main insight given by the present study is that the use of the pyrocarbon PIP implant changes manifold the magnitude of bone strains between intact and implanted states. Therefore, there is a potential risk of the support cancellous bone suffer fatigue failure in mid to long term due to the strain increase for cyclic loads in the range of daily hand activities, this risk is more prominent than the risk of bone resorption due to strain-shielding effect.

Acknowledgements

The authors wish to thank: Program COMPETE funding through the projects POCI-01-0145-FEDER-016574, PTDC/EMS-TEC/3263/2014 and Projecto 3599 – PPCDT e comparticipado pelo Fundo Comunitário Europeu FEDER e Fundação para a Ciência e Tecnologia (FCT).

References

Adkinson, J.M., Chung, K.C., 2014. Advances in Small Joint Arthroplasty of the Hand. Plast Reconstr Surg. 134, 1260–1268.

An, K.N., Chao, E.Y., Cooney, .WP., Linscheid, R.L., 1985. Forces in the normal and abnormal hand. J Orthop Res. 3, 202-211.

ASTM F1839-08, 2012. Standard Specification for Rigid Polyurethane Foam for Use as a Standard Material for Testing Orthopaedic Devices and Instruments, ASTM International, West Conshohocken, PA.

Branam, B.R., Tuttle, H.G., Stern, P.J., Levin, L., 2007. Resurfacing arthroplasty versus silicone arthroplasty for proximal interphalangeal joint osteoarthritis. J Hand Surg Am. 32, 775-788.

Bravo, C.J., Rizzo, M., Hormel, K.B., Beckenbaugh, R.D., 2007. Pyrolytic carbon proximal interphalangeal joint arthroplasty: results with minimum two-year follow-up evaluation. J Hand Surg Am. 32, 1-11.

Burstein, A.H., Wright, T.M., 1994. Fundamentals of Orthopaedic Biomechanics, Baltimore Williams&Wilkins, 191–217.

Ceruso, M.,, Pfanner, S., Carulli, C., 2017. Proximal interphalangeal (PIP) joint replacements with pyrolytic carbon implants in the hand. EFORT Open Rev. 13, 21-27.

Chan, K., Ayeni, O., McKnight, L., Ignacy, T.A., Farrokhyar, F., Thoma, A., 2013. Pyrocarbon versus silicone proximal interphalangeal joint arthroplasty: a systematic review. Plast Reconstr Surg. 131, 114-124.

Choi, K., Goldstein, S.A., 1992 A comparison of the fatigue behavior of human trabecular and cortical bone tissue. J Biomech. 25:1371-1381.

Chung, K.C., Ram, A.N., Shauver, M.J., 2009. Outcomes of pyrolytic carbon arthroplasty for the proximal interphalangeal joint. Plast Reconstr Surg. 123, 1521-1532.

Completo, A., Rego, A., Fonseca, F., Ramos, A., Relvas, C., Simões, J.A., 2010. Biomechanical evaluation of proximal tibia behaviour with the use of femoral stems in revision TKA: an in vitro and finite element analysis. Clin Biomech. 25, 159-65.

Completo A, Pereira J, Fonseca F, Ramos A, Relvas C, Simões J. 2011. Biomechanical analysis of total elbow replacement with unlinked iBP prosthesis: an in vitro and finite element analysis. Clin Biomech. 26, 990-7.

Completo A, Duarte R, Fonseca F, Simões JA, Ramos A, Relvas C. 2013. Biomechanical evaluation of different reconstructive techniques of proximal tibia in revision total knee arthroplasty: An in-vitro and finite element analysis. Clin Biomech. 28, 291-8.

Completo, A., Simões, J., Fonseca, F., 2008. Experimental Evaluation of Strain Shielding in Distal Femur in Revision TKA. Experimental Mechanics. 48, 817–824.

Cook, S.D., Beckenbaugh, R.D., Redondo, J., Popich, L.S., Klawitter, J.J., Linscheid, R.L., 1998. Long-term follow-up of pyrolytic carbon metacarpophalangeal implants. J Bone Joint Surg. 81, 635–648.

Daecke, W., Kaszap, B., Martini, A.K., Hagena, F.W., Rieck, B., Jung, M., 2012. A prospective, randomized comparison of 3 types of proximal interphalangeal joint arthroplasty. J Hand Surg Am. 37, 1770-1779.

Desai, A., Gould, F.J., Mackay, D.C., 2014. Outcome of pyrocarbon proximal interphalangeal joint replacement. Hand Surg. 19, 77-83.

Dickson, D.R., Nuttall, D., Watts, A.C., Talwalkar, S.C., Hayton, M., Trail, I.A., 2015. Pyrocarbon Proximal Interphalangeal Joint Arthroplasty: Minimum Five-Year Follow-Up. J Hand Surg Am. 40, 2142-2148.

Drake, M.L., Segalman, K.A., 2010. Complications of small joint arthroplasty. Hand Clin. 26, 205-212.

Fowler, N.K., Nicol, A.C., 2000. Interphalangeal joint and tendon forces: normal model and biomechanical consequences of surgical reconstruction. J Biomech. 33, 1055-1062.

Fok, K.S., Chou, S.M., 2010. Development of a finger biomechanical model and its considerations. J Biomech. 43, 701-713.

Frost, H.M., 2003. Bone's mechanostat: a 2003 update. Anat Rec A Discov Mol Cell Evol Biol. 275: 1081-1101.

Grant, J.A., Bishop, N.E., Götzen, N., Sprecher, C., Honl, M., Morlock, M.M., 2007. Artificial composite bone as a model of human trabecular bone: the implant-bone interface. J Biomech. 40, 1158-1164.

Gross, T.S., Rubin, C.T., 1995. Uniformity of resorptive bone loss induced by disuse. J. Orthop. Res. 13: 708-714.

Haugen, I.K., Englund, M., Aliabadi, P., Niu, J., Clancy, M., Kvien, T.K., Felson, D.T., 2011. Prevalence, incidence and progression of hand osteoarthritis in the general population: the Framingham Osteoarthritis Study. Ann Rheum Dis. 70, 1581-1586.

Heiner, A., 2008. Structural properties of fourth-generation composite femurs and tibias. J. Biomech. 41, 3282–3284.

Hutt, J.R., Gilleard, O., Hacker, A., Citron, N., 2012. Medium-term outcomes of pyrocarbon arthroplasty of the proximal interphalangeal joint. J Hand Surg Eur Vol. 37, 497-500.

Leuer, L.H., Gross, J.M., Johnson, K.M., 1996. Material properties, biocompatibility, and wear resistance of the Medtronic pyrolytic carbon. J Heart Valve Dis. 5, S105–S109.

Ma, L., Sines, G., 2000. Fatigue behavior of pyrolytic carbon, J Biomed Mat Res. 51, 61:68.

Mashhadi, S.A., Chandrasekharan, L., Pickford, M.A., 2012. Pyrolytic carbon arthroplasty for the proximal interphalangeal joint: results after minimum 3 years of follow-up. J Hand Surg Eur Vol. 37, 501-505.

McGuire, D.T., White, C.D., Carter, S.L., Solomons, M.W., 2012. Pyrocarbon proximal interphalangeal joint arthroplasty: outcomes of a cohort study. J Hand Surg Eur Vol. 37, 490-496.

Meireles, S., Completo, A., Simões, J., Flores, P., 2010. Strain shielding in distal femur after patellofemoral arthroplasty under different activity conditions. J Biomech. 43, 477-484.

Ono, S., Shauver, M.J., Chang, K.W., Chung, K.C., 2012. Outcomes of pyrolytic carbon arthroplasty for the proximal interphalangeal joint at 44 months' mean follow-up. Plast Reconstr Surg. 129, 1139-1150.

Reissner, L., Schindele, S., Hensler, S., Marks, M., Herren, D.B., 2014. Ten year follow-up of pyrocarbon implants for proximal interphalangeal joint replacement. J Hand Surg Eur Vol. 39, 582-586.

Squitieri, L., Chung, K.C., 2008. A systematic review of outcomes and complications of vascularized toe joint transfer, silicone arthroplasty, and PyroCarbon arthroplasty for posttraumatic joint reconstruction of the finger. Plast Reconstr Surg. 121, 1697-1707.

Stanley, J., Klawitter, J., More, R., 2008. Replacing joints with pyrolytic carbon. Joint Replacement Technology, pp. 631-656.

Sweets, T.M., Stern, P.J., 2011. Pyrolytic carbon resurfacing arthroplasty for osteoarthritis of the proximal interphalangeal joint of the finger. J Bone Joint Surg Am. 93, 1417-1425.

Surgical technique Ascension PIP Total Joint Replacement, Ascension Orthopedics, 2016

Watts, A.C., Hearnden, A.J., Trail, I.A., Hayton, M.J., Nuttall, D., Stanley, J.K., 2012. Pyrocarbon proximal interphalangeal joint arthroplasty: minimum two-year follow-up. J Hand Surg Am. 37, 882-888.

LIST OF FIGURES

Table 1 – Load cases analysed

Load case	Isometric hand activity	Joint angle	Joint force
1	Tip Pinch	50°	105 N
2	Key Pinch	35°	180 N
3	Pulp Pinch	15°	144 N
4	Tip Pinch	50°	465 N
5	Key Pinch	35°	868 N
6	Pulp Pinch	15°	481 N

Table 2 - Material properties used in the FE models.

Components	Material	Elastic modulus (GPa)	Poisson's ratio
Cortical bone	Composite material	16.7	0.3
Cancellous bone	Polyurethane foam	0.155	0.3
PIP implant componets	Pyrocarbon	29.4	0.28

Table 3 - P-values from T-tests, performed to test the difference of mean of cortex strains between implanted and intact PIP joint.

Strain gauge	Proximal Dorsal (Pr_D)		Proximal Palmar (Pr_P)		Middle Dorsal (Mi_D)		Middle Palmar (Mi_P)	
Principal Strain	ε2 (minimal)	ε1 (maximal)	ε2 (minimal)	ε1 (maximal)	ε2 (minimal)	ε1 (maximal)	ε2 (minimal)	ε1 (maximal)
Load case 1	p<0.05	p<0.05	p<0.05	0.06	p<0.05	p<0.05	p<0.05	0.11
Load case 2	p<0.05	0.10	p<0.05	0.21	p<0.05	p<0.05	p<0.05	0.09
Load case 3	p<0.05	p<0.05	p<0.05	p<0.05	p<0.05	p<0.05	p<0.05	p<0.05
Load case 4	p<0.05	p<0.05	p<0.05	p<0.05	p<0.05	p<0.05	p<0.05	0.12
Load case 5	p<0.05	0.12	p<0.05	p<0.05	p<0.05	p<0.05	p<0.05	0.08
Load case 6	p<0.05	p<0.05	p<0.05	0.07	p<0.05	p<0.05	p<0.05	0.06

Table 4 - Peak values of von Mises stresses in pyrocarbon componets.

Load case	Load case 1	Load case 2	Load case 3	Load case 4	Load case 5	Load case 6
von Mises peak stress (MPa)	5.3	14.2	7.9	21.8	66,8	24,7

FIGURES:

Figure 1

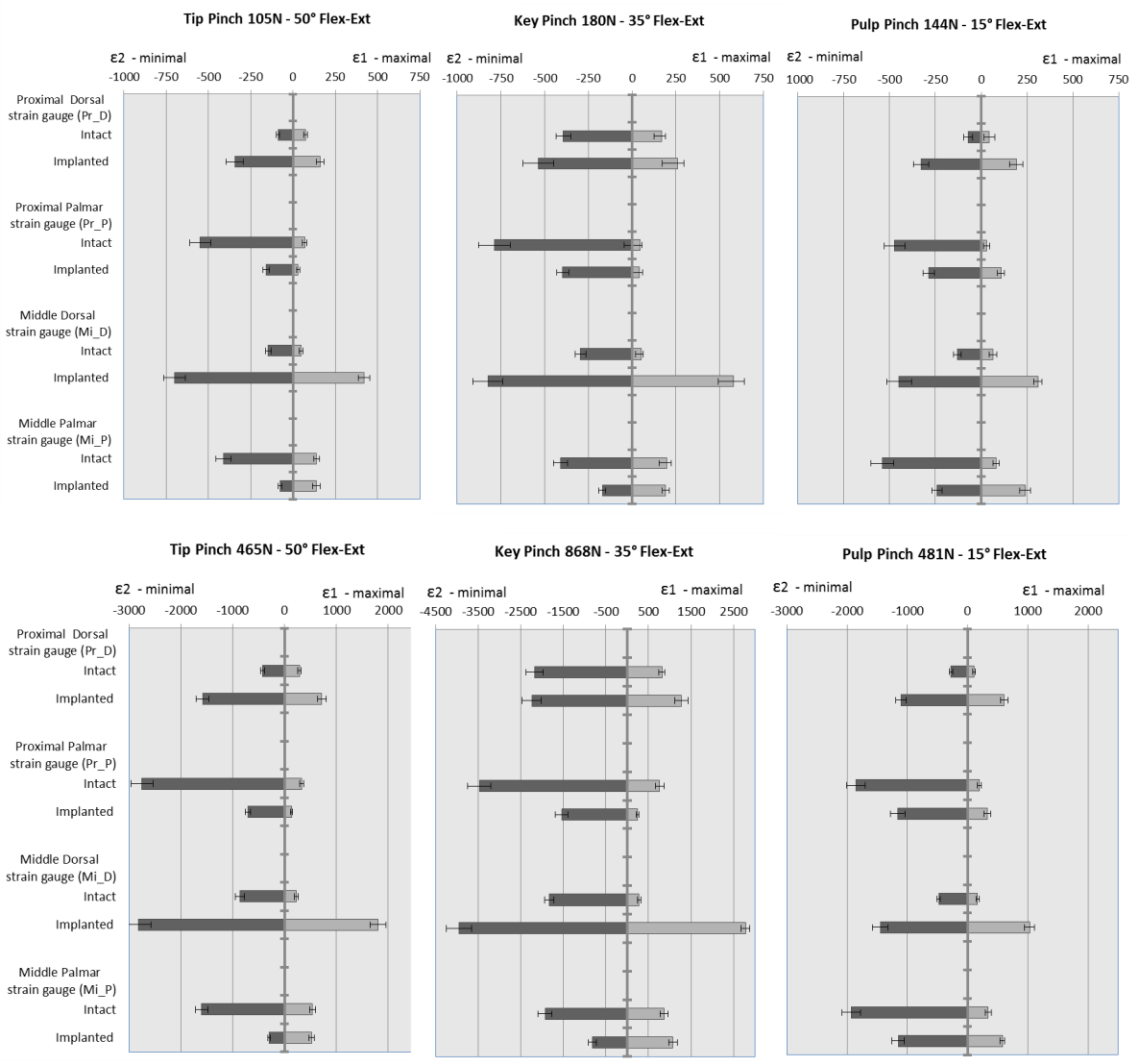

Figure 2

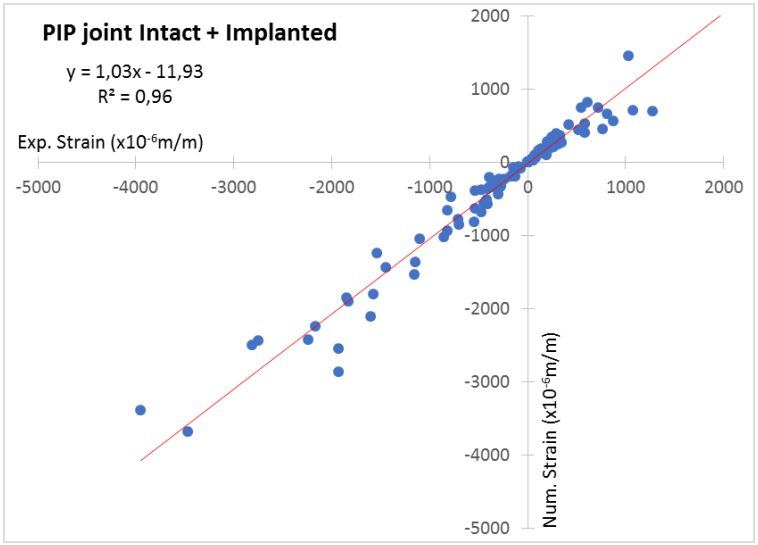

Figure 3

Load Case	Intact	Implanted
Pulp Pinch 144N – 15^0 Flex-Ext µstrain 0 -500 -1000 -1500 -2000 -2500 -3000 -3500 -4000 -4500 -5000	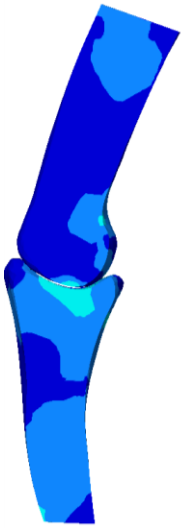	
Key Pinch 868N – 35^0 Flex-Ext µstrain 0 -2500 -5000 -7500 -10000 -12500 -15000 -17500 -20000 -22500 -25000	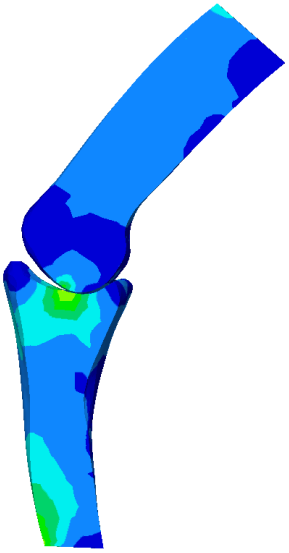	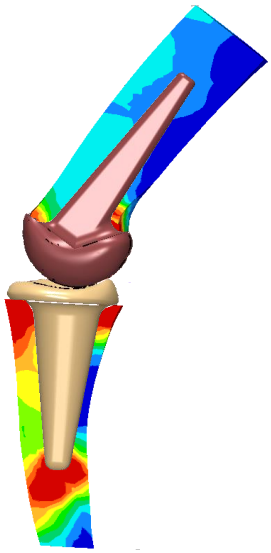
Tip Pinch 465N - 50^0 Flex-Ext µstrain 0 -1500 -3000 -4500 -6000 -7500 -9000 -10500 -12000 -13500 -15000	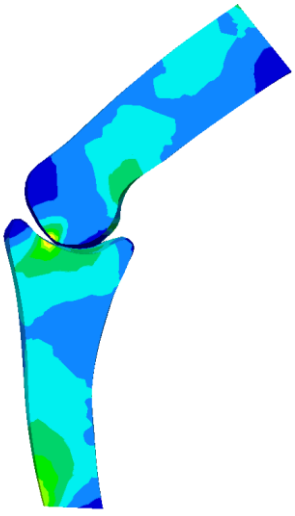	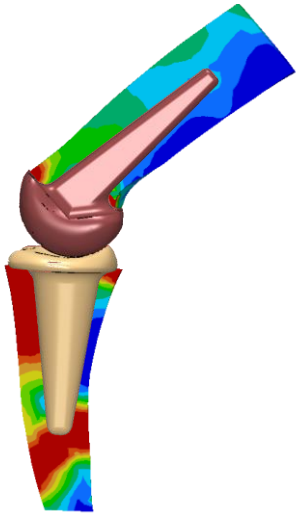

Figure 4